Published in final edited form in Biochemical Journal, 470 (3): 357-367 at https://doi.org/10.1042/BJ20150643.

A unique serpin P1' glutamate and a conserved β-sheet C arginine are key residues for activity, protease recognition and stability of serpinA12 (vaspin)

Short title: Molecular basis of vaspin activity, specificity and stability

David Ulbricht[*], Jan Pippel[†], Stephan Schultz[*], René Meier[*], Norbert Sträter[†] and John T. Heiker[*‡]

[*] Institute of Biochemistry, Faculty of Biosciences, Pharmacy and Psychology, University of Leipzig, 04103 Leipzig, Germany
[†] Center for Biotechnology and Biomedicine, Institute of Bioanalytical Chemistry, University of Leipzig, 04103 Leipzig, Germany

[‡] Corresponding author:
Dr. Dr. John T. Heiker
E-mail: jheiker@uni-leipzig.de
Institute of Biochemistry
Leipzig University
Brüderstrasse 34
04103 Leipzig, Germany
Tel.: +49-341-9736705
Fax: +49-341-9736909

Keywords: adipokine, exosite, kallikrein 7, reactive center loop, serpin, vaspin

Abbreviations: AT: antithrombin; GAG: glucosaminoglycan; KLK7: human kallikrein 7; RCL: reactive center loop; s2C: β-sheet C; UFH: unfractionated heparin

Summary: We investigated the influence of reactive center loop and neighboring residues on protease inhibition and stability of vaspin. We found that while Glu^{379} severely depresses activity, Arg^{302} as a crucial contact enables moderate inhibitory activity and further hinders vaspin polymerization.

Abstract
SerpinA12 (vaspin) is thought to be mainly expressed in adipose tissue and has multiple beneficial effects on metabolic, inflammatory and atherogenic processes related to obesity. Kallikrein 7 (KLK7) is the only known protease target of vaspin to date and is inhibited with a moderate inhibition rate. In the crystal structure, the cleavage site (P1-P1') of the vaspin reactive center loop is fairly rigid compared to the flexible residues before P2, possibly supported by an ionic interaction of P1' glutamate (Glu^{379}) with an arginine residue (Arg^{302}) of the β-sheet C. A P1' glutamate seems highly unusual and unfavorable for the protease KLK7. We characterized vaspin mutants to investigate the roles of these two residues in protease inhibition and recognition by vaspin. RCL mutations changing the P1' residue or altering RCL conformation significantly increased inhibition parameters while removal of the positive charge within β-sheet C impeded the serpin-protease interaction. Arg^{302} is a crucial contact to enable vaspin recognition by KLK7 and it supports moderate inhibition of the serpin despite the presence of the detrimental P1' Glu^{379}, which clearly represents a major limiting factor for vaspin inhibitory activity. We also show that the vaspin inhibition rate for KLK7 can be modestly increased by heparin and demonstrate that vaspin is a heparin-binding serpin. Noteworthy, we observed vaspin as a remarkably thermostable serpin and found residues Glu^{379} and Arg^{302} influencing heat-induced polymerization. These structural and functional results reveal the mechanistic basis of how reactive center loop sequence and exosite interaction in vaspin enable KLK7 recognition and regulate protease inhibition as well as stability of this adipose tissue derived serpin.

Introduction
SerpinA12 (vaspin) is an inhibitory serpin first identified in white adipose tissue of the OLETF rat type-2 diabetes model [1]. In humans, elevated vaspin mRNA and serum levels are associated with parameters of obesity and insulin resistance [2, 3]. Vaspin is a promising drug target with various beneficial effects on metabolic and atherogenic processes impaired or induced in overweight and obesity [4]. It has been suggested to function as a compensatory, anti-diabetic and anti-atherogenic protein in obesity related disorders such as insulin resistance and inflammation [5]. Under a high fat diet, vaspin transgenic mice gain less weight while exhibiting improved glucose tolerance and reduced adipose tissue inflammation [6]. Also central effects have been reported and central administration of vaspin reduced food intake in mice [7]. Kallikrein 7 (KLK7) is the only known protease target of vaspin by now and at least the beneficial effects on glucose tolerance *in vivo* are dependent on the protease inhibitor activity of vaspin [8]. KLK7 seems to be mainly expressed in skin where it is a key player in the desquamation of cornified skin layers [9]. Both proteins, KLK7 and vaspin, are reported to be involved in skin inflammation as in psoriasis, a chronic skin disease often related to obesity [10, 11]. KLK7 overexpressing mice exhibit increased epidermal thickness, hyperkeratosis, and dermal inflammation [12, 13]. In humans, elevated *KLK7* mRNA as well as KLK7 protein overexpression has been reported in various tumors such as ovarian, breast and cervical cancer [14-16]. Along these lines, a better understanding of vaspin function and regulation on a molecular level might lead to new strategies for pharmaceutical intervention or modulation of vaspin activity.
Serpins inhibit protease targets using their reactive center loop (RCL) as substrate bait. After protease attack and acyl-enzyme complex formation, the protease-bound RCL integrates into the central serpin β-sheet, thereby causing active-site distortion and preventing hydrolysis, final cleavage and release of the protease. The primary determinants of serpin specificity are the cleavage site and surrounding residues of the RCL. The crystal structure of human vaspin in its native conformation has been previously determined [8]. Vaspin exhibits interesting molecular aspects. As many other inhibitory serpins, vaspin exhibits a mostly flexible reactive center loop (RCL) unresolved in the crystal structure. The protease cleavage site appears more rigid compared to other serpin structures, possibly due to ionic interactions of P1' Glu^{379} and Arg^{302} of the β-sheet C in the crystal structure (Figure 1A). First of all, the highly unusual glutamate residue at the P1' position of the protease cleavage site, which is unique amongst all human serpins, indicates functional relevance, particularly as the protease target KLK7 has a clear preference for basic residues at P1' [17]. This might explain the moderate association rate and a comparatively high stoichiometry of inhibition observed for vaspin and KLK7 [8]. Also, Arg^{302}, a well conserved residue in the serpin family, has been found to be of importance for protease recognition in other serpins [18, 19]. Here, we used a mutational approach to determine the influence of these two residues on KLK7 inhibition and on vaspin stability. Our results demonstrate the significant, yet opposing impact of both residues on vaspin activity. While P1' Glu^{379} is an obvious down-regulator of

vaspin inhibitory activity, Arg^{302} represents a critical contact for KLK7 and enables a moderate inhibition rate for KLK7, potentially by offsetting the limitations of the unfavorable RCL sequence. Based on these results and properties from other serpins, we also investigated the possible activation of vaspin by heparin and found significant heparin-binding with a modest activation of vaspin. On a further note, investigating structural serpin parameters, we registered vaspin as a remarkably thermostable serpin and found both residues, Arg^{302} and Glu^{379}, influencing serpin polymerization.

Materials and methods

Materials Human recombinant KLK7 and thermolysin were from R&D (Minneapolis, MN). Fluorogenic peptide substrate Mca-RPKPVE-Nva-WR-K(Dnp)-NH2 was from AnaSpec (Fremont, CA) and the substrate peptide Abz-KLYSSK-Q-EDDnp was a generous gift of Prof. Dr. Maria A. Juliano (Department of Biophysics, Escola Paulista de Medicina, Universidade Federal de São Paulo, Brazil). Human antithrombin III (AT) purified from human plasma was obtained from Thermo Fischer Scientific (Rockford, IL). Unfractionated heparin (ufh) was from Sigma-Aldrich, heparin oligosaccharide dp4 was from Iduron (Manchester, UK). All calculations were done using Prism 5.03 (GraphPad Software).

Generation of recombinant vaspin and KLK7 proteins Mutagenesis, recombinant expression and purification of vaspin and mutants was carried out as previously described with minor changes [8]. Disulfide bond containing mutants were dialyzed using an L-cysteine/-cystamine redox system (5 mM/1 mM). A polishing gel filtration step was performed after final dialysis using a HiLoad 16/60 Superdex 200 column on an ÄKTA protein purification system (all from GE Healthcare, Freiburg, Germany). Purified proteins were analyzed by RP-HPLC, SDS-PAGE as well as MALDI-TOF mass spectrometry and were stored at 4 °C for up to one year without loss of activity. Recombinant expression and purification of KLK7 will be published in full detail elsewhere. Briefly, KLK7 was expressed as a fusion to the small ubiquitin-like modifier (SUMO) protein as inclusion bodies in *E. coli.* The fusion protein was refolded from guanidine by fast dilution in an arginine-glycerol buffer supplemented with a glutathione redox system. The SUMO protein was cleaved off with SUMO protease and purification of active KLK7 was performed using a HiTrap SP HP column followed by a final gel filtration step using a HiLoad 16/60 Superdex 200 column. Enzyme activity of recombinant KLK7 was comparable to commercially available KLK7 using the fluorogenic peptide Mca-RPKPVE-Nva-WR-K(Dnp)-NH2.

Crystallization, X-ray data collection and structure determination For crystallization, gel filtration peak fractions were pooled and concentrated to 12 mg/ml. In a hanging-drop vapor diffusion setup at 292 K, 1 µl protein and 1 µl crystallization buffer were mixed and equilibrated against 0.5 ml of crystallization buffer as reservoir solution. The analyzed crystals were transferred stepwise to a buffer containing 20% ethylene glycol in addition to the components in the crystallization buffer and frozen in liquid nitrogen. X-ray data collection was carried out at 100 K on beamline 14.1 of the Berlin Synchrotron (BESSY, Berlin, Germany) equipped with a PILATUS 6M detector (Dectris, Baden, Switzerland). The diffraction data were indexed, integrated and scaled with XDS [20] and aimless [21] of the CCP4 suite [22]. Coordinates from wild-type vaspin (pdb 4IF8) were taken as starting models for rigid body refinement in REFMAC5 [23, 24]. Models were further improved by iterative cycles of TLS refinement using REFMAC5 [23, 24] as well as BUSTER-TNT [25] and manual rebuilding with COOT [26]. The artificial disulfide bridge of chain A in the variant D305C/V383C was refined with an occupancy of 25 % in the reduced form. Reduction of the disulfide linkage could be unambiguously ascribed to radiation damage by using only the first 40 % of the data set (yielding a data completeness of 97.9 %) for refinement. With this data set the electron density showed no evidence for an open conformation of the disulfide bridge. In chain B, no alternative conformation was observed for the artificial disulfide bridge. We attribute this to the generally lower quality of the electron density of this chain, which is accompanied by significantly higher B-factors, most likely as a resulted of static disorder of this protein chain in the crystal. TLS groups (chain A: residues 36-70, 71-242, 243-308 and 309-414; chain B: residues 36-70, 71-176, 177-303, 304-413) were determined using the TLSMD web server [27, 28]. Structures were validated by MOLPROBITY [29]. Final structure building and interpretation was aided by feature enhanced maps calculated with PHENIX [30, 31]. For crystallization of the E379S variant, a heparin tetrasaccharide was added to the crystallization buffer but no binding of the heparin was observed in the electron density maps. Crystals obtained in the absence of heparin showed identical

features (data not shown). Final coordinates and structure factors have been deposited in the Protein Data Bank (www.rcsb.org [32]) under accession codes 4Y3K (E379S) and 4Y40 (D305C/V383C) and relevant crystallographic data is specified in Table 1. Figures were prepared using PyMOL (www.pymol.org).

Inhibition parameters. The stoichiometry of inhibition (SI) was determined as previously described [8]. A discontinuous assay was used to determine the rate of inhibition under pseudo-first order conditions for vaspin wild-type and mutants D305C/V383C, R302A, R302E, R302E/E379S with at least 10-fold molar excess of inhibitor, as previously described [33]. Briefly, recombinant human KLK7 was activated according to the manufacturers' protocol and the assay concentration of KLK7 was 19.2 nM in TBS buffer (50 mM Tris, 150 mM NaCl, pH 8.5). Inhibition reactions were stopped by addition of fluorogenic peptide substrate (30 µM) and residual KLK7 activity was measured on a FlexStation3 Multi-Mode Microplate Reader (Molecular Devices, Sunnyvale, CA). The pseudo-first-order rate constant (k_{obs}) was obtained from linear regression of semi-logarithmic plots of remaining KLK7 activity vs. time. Linear regression of k_{obs} plotted against inhibitor concentration [I] resulted in the estimate of the second-order rate constant, k_a.
A continuous method was used to determine the rate of inhibition for vaspin mutant E379S with at least 5-fold molar excess of inhibitor, as previously described [34]. The assay concentration of KLK7 was 10 nM, the fluorogenic peptide was used at 25 µM. Here, k_{obs} was determined by non-linear regression fitting of the progress curve to equation 1:

$$P = \frac{v_0}{k_{obs}}[1 - e^{-k_{obs} \times t}]$$

P is the concentration of product at the time t and v_o is the initial velocity for each [I]. Resulting k_{obs} values were plotted against [I] and the uncorrected second-order rate constant k' was determined from the slope of linear fit. Finally, the second order rate constant, k_a, was calculated by correcting k' for substrate concentration [S], the K_M of the protease and SI using equation 2:

$$k_a = k' \times (1 + \frac{[S]}{K_M}) \times SI$$

The K_M value for KLK7 was 15 µM. SI values and inhibition rates listed in Table 2 represent the average of at least three experiments from at least two protein batches.
The pseudo-first-order rate constant (k_{obs}) was furthermore determined in the presence of various concentrations of ufh (ufh:vaspin ratios of 1,56-, 12,5- and 100-fold) using the discontinuous method with 10-fold molar excess of inhibitor to maintain pseudo-first-order conditions. In these assays, the substrate peptide Abz-KLYSSK-Q-EDDnp [17] was used at a concentration of 7 µM. k_{obs} values indicating for reaction speed were normalized to the reaction without ufh to estimate the relative heparin induced increase in activity.

Complex formation analysis by SDS-PAGE To investigate complex formation, recombinant KLK7 and vaspin, or mutants, were incubated at a ratio of 3:1 (protease:serpin; KLK7 concentration was 3.5 µM) in TBS buffer (50 mM Tris, 150 mM NaCl, pH 8.5). At given time points samples containing 0.5 µg of serpin were taken and the reaction was stopped by immediate addition of reducing SDS sample buffer and 5 min of heating at 95 °C. Protein separation by SDS-PAGE was performed using 4-12% Bis-Tris Plus precast gels and NuPAGE MES/SDS running buffer (all from Life Technologies, Carlsbad, CA). Gels were stained with Coomassie Blue, digitization and densitometric analysis were performed using GeneTools analysis software (Syngene). Estimation of SI values were calculated as the sum of band intensities for complexed and cleaved vaspin divided by the band intensity of complexed vaspin [35]. To analyze the effect of heparin on the vaspin-KLK7 reaction, complex formation assays were performed as described above with various concentrations of ufh (molar ratios of heparin to vaspin from 0.1 – 100) and the reactions were stopped after 1 min of incubation. Complex band intensities were then normalized to the reaction without heparin.

Heparin affinity chromatography 200 µg of recombinant protein was used for heparin affinity chromatography with 1ml HiTrap Heparin HP columns on the ÄKTA protein purification system (both from GE Healthcare, Freiburg, Germany). Elution was performed by a sodium chloride gradient from 150 mM to 2 M (flow rate: 1 ml/min) and monitored at 220 nm.

Thermal stability Circular dichroism (CD) spectra were recorded using 1 mm quartz cuvettes (Hellma, Jena, Germany) on a J-715 spectropolarimeter (Jasco, Tokyo, Japan) equipped with a Peltier-type temperature control system at 20 °C. Spectra were acquired as an average of three scans (2 nm bandwidth, 4 s response, 50 nm/min scan rate) and base-lines were corrected by subtraction of the buffer spectrum. The protein concentration was 1.5 µM in 10 mM phosphate buffer, pH 7.8. Thermal unfolding was performed at a heating rate of 50 °C/h and monitored at 208 nm (data pitch 0.1 °C, sensitivity 100 mdeg, 4 s response, band width 2 nm). Measured ellipticity θ was converted to mean residue molar ellipticity [θ] in $deg \cdot cm^2 \cdot dmol^{-1}$ as previously described [36].

Temperature induced polymerization 5 µM of antithrombin (AT), vaspin or mutants were heated for 120 min at 60 °C or 70 °C in TBS buffer. During heating, samples were taken at indicated time points and non-reducing SDS-sample buffer was added. Vaspin-KLK7 complex formation after heating was analyzed as described above, with 2 min cooling on ice before incubation with KLK7 for 15 min. Polymerization and complex formation were analyzed by SDS-PAGE.

Peptide synthesis and RP-HPLC based analysis of KLK7 cleavage Peptide synthesis, purification and analytics were performed as previously described [10]. For cleavage analysis, 250 µg vaspin(365-388) was incubated with 2 µg KLK7 (327 nM) in a 250 µl reaction volume for 120 min at 37 °C. After incubation, proteolytic activity was terminated by boiling and the peptide mixtures were analyzed by RP-HPLC (Phenomenex Jupiter Proteo C18 column, 4.6 mm×250 mm, 90 Å pore size).

Results

Altering vaspin RCL constraints via two designed variants

Vaspin and its mutants crystallize in space group C2 with two monomers in the asymmetric unit (Table 1). Although no systematic differences are observed between the two molecules, in monomer B the lack of crystal contacts results in a rigid body disorder of the whole subunit such that the regions close to the interaction interface with monomer A have low B-factors and well defined density and the complete subdomain comprising sheet 3 and the RCL exhibit high B-factors and ill-defined density (Supplementary Figure 1A, B). As a result, the density of the RCL and nearby regions is less well-defined and fewer residues of the RCL could be modeled, including residues involved in the interactions described below. Since this is a result of a rigid body disorder of the whole subunit, these interactions are likely to be present but they are not evident by the electron density maps which are affected by the rigid body disorder. Therefore, the following observations, figures and calculations are based on chain A.

In the crystal structure, the P1' Glu^{379} forms a weak salt bridge with the side chain of Arg^{302} within strand 2 of β–sheet C (s2C) and water-mediated hydrogen bonds with the main chain CO of Arg^{301}. Also P2' Thr^{380} interacts with the Arg^{302} side chain via a water-mediated hydrogen bond (Figure 1A). Collectively, these interactions could limit the overall flexibility of the C-terminal part of the RCL with the cleavage site. Noteworthy, RCL orientations in serpin crystal structures display great variability and do not necessarily represent the conformation of the free serpin in solution.

We aimed to alter the cleavage site by mutating the P1' glutamate to serine, a very common P1' residue in the serpin family (E379S mutant) [37]. Also, a recent study investigated the primed subsite (S1'-S3') preferences of KLK7 and demonstrated a clear P1' preference for hydrophilic residues, especially arginine and serine [17]. To specifically dissect the effect of RCL flexibility or conformation from P1' specificity of KLK7, we furthermore designed a variant, where we introduced a disulfide linkage at the C-terminal side of the cleavage site via the D305C/V383C double mutant. This disulfide bridge was intended to induce an altered RCL conformation while the native RCL sequence with respect to protease substrate specificity is preserved.

Overall, the crystal structures of both mutants show no conformational differences to wild-type vaspin further away from the mutation sites, as demonstrated by r.m.s. deviations of 0.38 Å (E379S) and 0.33 Å (D305C/V383C) calculated for the Cα atoms of chain A. The RCL hinge region of residues P15 to P13/P12 (residues 364-366/367) is well-defined and extends away from the central β–sheet A. In contrast, the electron density for RCL residues P12/P11-P2 (G^{367}/A^{368}-P^{377}) and the N-terminal RCL part is weak or absent indicating high flexibility in both structures, similar to the situation in wild-type vaspin (Supplementary Figure 1C). The only exception concerns RCL residues P1-P2' (Met^{378} – Thr^{380}). As mentioned above, in wild-type vaspin these residues are rather well defined (Figure 1A), but there is

weak ambiguous electron density in the E379S mutant structure indicating also a very flexible C-terminal RCL (Figure 1B). In the D305C/V383C mutant, formation of the engineered disulfide bond was verified by the electron density maps (Figure 1C) and resulted in a band with a distinct shift on a non-reducing SDS gel, confirming full formation of the disulfide bond (Supplementary Figure 2). Comparable to the E379S mutant, the P1 and P1' residues (Met^{378} and Glu^{379}) also exhibit only weak electron density and thus are much more flexible compared to the wild-type vaspin structure (Figure 1C). Hence, the successful introduction of the artificial disulfide linkage was sufficient to alter RCL conformation and both mutant structures exhibit less constrained RCLs.

Change of RCL sequence and conformation results in accelerated and more efficient KLK7 inhibition

Both, the introduction of the disulfide bond and P1' exchange, resulted in significant improvement in serpin activity (Table 2). As expected, exchange of the P1' residue in the E379S variant resulted in a dramatic rate acceleration of ~35-fold, requiring a change to a continuous assay, while all other mutants were characterized in a discontinuous assay (Table 2, Figure 2A). Also the D305C/V383C mutant exhibits a significant ~4.5-fold increase in KLK7 inhibition rate (Table 2, Figure 2B). This mutant features the native RCL sequence and thus the effect is independent of substrate specificity of KLK7. The SI measured for both vaspin mutants was ~2 (Table 2, Figure 2C).

These results are also reflected in accelerated complex formation observed in SDS-PAGE analysis for both mutants (Figure 3A). The native RCL sequence seems to prevent a fast protease attack. After 60 min almost all serpin molecules are either cleaved or complexed for both mutants, whereas ~25% of wild-type vaspin remains unaffected after 120 min (Figure 3A). In conclusion, mutation of the P1' residue Glu^{379} to the more preferred serine demonstrates the explicit rate-reducing effect of the native P1' residue in this system. Yet, an alteration of the RCL conformation could also moderately improve serpin activity despite the detrimental P1' Glu^{379}.

Elimination of the positive charge at position 302 reveals a crucial contact for KLK7 recognition

Since conformational alterations as induced by the disulfide-mutant increased vaspin inhibition rates, we investigated the existence of further determinants of activity and specificity in addition to the P1' residue. We analyzed the importance of Arg^{302} in KLK7 inhibition by vaspin. This positively charged residue is well conserved throughout the serpin family and the orientation of the side chain is in good superposition in many serpin structures (Supplementary Figure 3). Furthermore, this arginine has been found to be a critical contact point in the Michaelis complex of heparin cofactor 2 (serpinD1) as well as thrombin [18], and is part of a basic exosite for the inhibition of tissue kallikrein by kallistatin (serpinA4) [19].

For vaspin, the mutation of arginine to alanine (R302A) resulted in dramatic loss of inhibitory activity (~40-fold) compared to wild-type (Table 2, Figure 2B). This is also evident in the very slow complex formation (Figure 3B). Introduction of a negatively charged glutamate (R302E) resulted in almost complete prevention of the serpin-protease interaction and no measurable inhibitory activity (Table 2, Figure 2B, 3B). After 16 h of incubation only faint bands of complexed and cleaved serpin were detected with ~90% serpin remaining active. These results are also in line with the finding, that a synthetic peptide comprising the vaspin RCL sequence, vaspin(365-388), is not cleaved by KLK7 (Figure 3C). Densitometric estimation of the SI for the R302A and R302E mutants indicated an SI comparable to the wild-type vaspin (Table 2). Mutation of the Arg^{302} in the disulfide bond mutant (R302A/D305C/V383C, R302E/D305C/V383C) resulted in a similar loss of activity and serpin-protease interaction as observed in wild-type vaspin (Table 2, Figure 3D). As expected, loss of Arg^{302} in the E379S mutant did not completely prevent inhibition of KLK7, as the RCL sequence is adjusted to KLK7 subsite preference, but still slowed down the reaction by >90% (Table 2, Figure 3D). In conclusion, Arg^{302} comprises a crucial residue for initial KLK7-vaspin Michaelis complex formation with subsequent cleavage site attack promoting the inhibition reaction and bypassing the repressing effect of P1' Glu^{379}.

Heparin activates vaspin and accelerates KLK7 inhibition

We further investigated whether heparin, a common activator of serpin activity, is able to bind and activate vaspin. Indeed, vaspin as well as KLK7 bound to heparin-sepharose and eluted at ~580 mM and ~420 mM NaCl in heparin-affinity chromatography experiments (Figure 4A). When evaluating the effect of heparin on vaspin activity, we found a concentration dependent increase of vaspin activity both,

by analyzing vaspin-KLK7 complex formation on SDS-PAGE gels (Figure 4B, C) and by measuring the inhibition rate for wt vaspin (Figure 4D). At the optimal ratio of heparin to vaspin (12.5-fold ufh in our experiments), we observed a modest ~5-fold increase in vaspin activity towards KLK7. The bell-shaped dose-response curve for heparin activation may indicate activation via the bridging mechanism for vaspin and KLK7 by heparin.

Thermo-stability and vaspin polymerization

Far-UV CD data reflected the structural similarity and demonstrated structural integrity for all mutants tested (Figure 5A). Thermal denaturation revealed a remarkable thermo-stability with temperature midpoints (T_m) of 70 °C and a well-defined isochromatic point suggests a two-state unfolding pathway progressing from the native to unfolded state (Figure 5B, C). Thermal unfolding seems irreversible and heat-induced aggregation and precipitation was observed. Vaspin was found considerably resistant to heat-induced inactivation by polymerization. Prolonged incubation of up to 120 min at 60 °C did not noticeably alter serpin activity analyzed via complex formation with KLK7 (Figure 5D). Also, polymers were almost undetectable in non-reducing, non-heated SDS-samples, whereas for AT, serving as a control, polymerization was apparent after 15 min at 60 °C (Figure 5E). As expected from the Tm values, increasing the temperature to 70 °C resulted in distinct vaspin polymer formation (Figure 5F). Polymerization was markedly enhanced in Arg^{302} deficient mutants and also observed for the disulfide mutant D305C/V383C. Polymerization for the E379S containing mutants was minor and alike the wild-type. In conclusion, vaspin represents a highly thermo-stable serpin and Arg^{302} seems to hinder polymer formation in wild-type variants featuring the native Glu^{379}.

Discussion

We have previously identified KLK7 as the first target protease of human vaspin inhibited with a moderate inhibition rate [8]. The RCL P1' Glu^{379} residue, unique amongst all human serpins, indicates functional relevance. By changing the RCL sequence or conformation, the first by mutation of Glu^{379}, the latter by an engineered disulfide bond, we observed increasing RCL flexibility in the crystal structures. Alongside, the mutants featured increased inhibition rates, with a far more pronounced increase in activity for the E379S mutant. This can be attributed to a much more preferred P1' serine residue over glutamate for KLK7. The primed subsite (S1'-S2') of KLK7 clearly prefers amino acids serine and arginine at the substrates P1' and P2' position and in a soluble peptide library P1' glutamate featuring peptide substrates were all found resistant to hydrolysis [17]. In accordance with these data, no cleavage of a synthetic peptide comprising the RCL sequence of vaspin by KLK7 was observed. Yet, the significant effect on activity of the disulfide-bond demonstrates a moderate contribution of RCL conformation or flexibility, as this mutant exhibits the native RCL sequence. Together, these results clearly reveal, that the P1' glutamate is detrimental to vaspins inhibitory activity and it may function as a regulatory element in reducing the inhibition rate.

Related to this, almost a complete loss of inhibition and interaction was observed when mutating the positively charged Arg^{302} within s2C for all variants featuring the P1' glutamate. The finding, that also the KLK7-adjusted RCL-mutant E379S loses ~90% of activity when lacking Arg^{302}, further demonstrates the importance of this residue for KLK7 recognition. Together with the specificity studies on KLK7, these results highlight the necessity of Arg^{302} for KLK7 inhibition by vaspin to offset the effect of the impedimental P1' glutamate and explain the moderate inhibitory activity of native vaspin observed for KLK7. In conclusion, Arg^{302} seems to represent a crucial contact for the serpin-protease interaction and its presence or access to it regulates whether or not the target protease KLK7 is inhibited at all. Thus, vaspin is an example of how serpins generate specificity via exosite interactions with their target proteases but at the cost of maximal inhibitory activity.

In kallistatin, Arg^{308}, the equivalent to vaspins Arg^{302}, is part of an exosite with tissue kallikrein that comprises a cluster of positively charged residues (K307A/R308A and K312A/K313A all in s2C). Mutations of these positively charged residues in kallistatin resulted in 5 to 20-fold lower activity [19]. In kallistatin, this exosite is supposed to enable specific inhibition of kallikreins despite the kallistatin P1 Phe residue being inappropriate for kallikreins. The exosite mutations in kallistatin were performed as double mutations and there is no data on the effect of individual mutations of single charged residues. While with Arg^{302} in vaspin, a single mutation almost completely prevents KLK7 recognition and subsequent inhibition, it is likely, that more residues contribute to KLK7 recognition and binding, e.g. the neighboring Arg^{301}, but also that other exosites are still to be identified.

In addition to exosites promoting binary complex formation of serpin and protease, there are also exosites involved in ternary complex formation with additional cofactors [38]. In light of the detrimental P1' Glu^{379}, we investigated if activity of vaspin could also be increased by cofactors, such as the glucosaminoglycan heparin. First, we found strong heparin binding for both vaspin and KLK7. Binding and activation of KLK7 by heparin has been previously reported, with KLK7 eluting at 0.3-0.4 mM NaCl from heparin-sepharose [17]. This is in line with our findings for the recombinant KLK7 used in our assays. Importantly, we also observed a modest, but distinct and concentration dependent heparin-induced increase in KLK7 inhibition by vaspin (~5-fold). It is important to note, that the heparin induced vaspin activation was quantified accounting and normalizing for any heparin induced increase in KLK7 activity, as KLK7 is also moderately activated by heparin (~2-fold at ~100-fold excess of GAG, [17]). The major contribution of GAG-activation of serpins comes via the template mechanism, i.e. bridging serpin and protease and directing a preferential orientation of protease and serpin RCL [38]. Also here, the bell-shaped dependence on heparin concentration suggests a bridging effect of heparin for vaspin activation, as very high GAG concentrations counteract the activating effect. Thus, vaspin is a heparin-binding, though very modestly heparin-activated serpin. Interestingly, while there are similarities in this exosite residue for the two serpins vaspin and kallistatin, heparin binding has opposing effects for their activity. For kallistatin, heparin binding occurs at the exosite comprising Arg^{308} and in consequence counteracts protease inhibition [39]. As heparin is able to activate vaspin, the binding site has to be located somewhere else, or at least Arg^{302} is not likely to contribute to GAG binding and we are currently working on the identification of the GAG binding site in vaspin.

Investigating the structural integrity of the generated mutants, we found vaspin to be remarkably thermostable, with a T_m of 70 °C compared to AT (T_m of 57 °C) or antitrypsin (T_m of 58 °C) [40, 41]. Thermopin, a thermostable serpin from the bacterium *Thermofibia fusca* has a T_m of 65 °C, enabling functionality at the preferred growth temperature of 55 °C [42]. The T_m was identical for all mutants tested. These data reveal no major thermodynamic importance of the potential interaction of Glu^{379} and Arg^{302} observed in the crystal structure and thus, further determinants are likely to contribute to the thermal stability of vaspin. Surprised by these findings, we were also interested in heat-induced polymerization for vaspin and variants. There are two pathways of serpin inactivation independent from protease attack, which are the latent transition and serpin polymerization. The transition into the latent conformation occurs via incorporation of the RCL into β-sheet A, as for example observed for PAI-1 or AT [43-45]. Based on crystal structure data, the hinge region of vaspin is not partially incorporated into the central A-sheet as e.g. in native AT and we also have not observed considerable loss of activity for vaspin stored at 4 °C for months. Thus, vaspin seems not prone to undergo the latent transition. Alternatively, serpins are able to polymerize and the mechanism thought to most likely represent the *in vivo* polymerization mechanism features a swap of major C-terminal domains involving strands s1C, s4B and s5B but RCL incorporation into the own central β-sheet A, as for the latent transition [46]. *In vivo*, serpin polymerization is observed for mutations affecting folding, formation and stability of the native state, e.g. for the Z variant (E342K) of antitrypsin [47]. A recent study concluded that these mutations likely first of all affect the stability of the metastable native state and ultimately facilitate or hinder the irreversible polymerization step [41]. Serpin polymerization is heat-inducible and elevated temperatures inactivate most inhibitory serpins due to polymerization [48]. For vaspin, the residues Arg^{302} and Glu^{379} seem to affect heat-induced polymerization. Mutants featuring the native Glu^{379} without Arg^{302} (R302A and R302E) polymerized more readily than the wild-type. In contrast, E379S containing mutants as well as mutation of Arg^{302} did not influence polymerization and were comparable to wild-type vaspin. Together, Glu^{379} seems to facilitate polymer formation, whereas Arg^{302} counteract and appears to stabilize vaspin as a monomer in the native state. On a side note, we were initially surprised to observe polymerization of the D305C/V383C mutant, as this disulfide bond should prevent extended RCL movement likely required for a domain-swap mechanism of polymerization. But recently, Irving et al. have also observed polymerization for a similarly disulfide-stabilized antitrypsin variant (S283C/P361C) [41].

In conclusion, our data revealed Glu^{379} and Arg^{302} as important regulatory elements for serpin functionality, such as protease specificity, activity and stability and explain the observed moderate activity for the target protease KLK7. Thereby, RCL P1' residue Glu^{379} is the down regulating element, whereas the exosite at Arg^{302} enables inhibition of KLK7 despite the obviously inappropriate P1' residue. The reason underlying this deliberate limitation of vaspin activity by Glu^{379} has to be further investigated. It very likely enhances specificity for KLK7, because inhibition of other proteases

preferring similar P1 residues could be even more negatively affected by the presence of this P1' residue. Vaspin serum concentrations are very low and positively correlated with increasing fat mass, obesity and insulin resistance [4]. An important function of vaspin is its positive effect on insulin action, as application or overexpression in mice improves glucose tolerance [1, 6]. We have demonstrated that this effect is dependent on vaspins inhibitory activity [8]. Also, vaspin expression follows a circadian rhythm and peak levels of vaspin precede post prandial insulin secretion peaks [49] and an acute insulin dose in humans rapidly decreases vaspin serum levels [50]. In addition to avoid potentially adverse influence on non-target protease-mediated processes, a high specificity and prevention of vaspin consumption due to interaction with non-target proteases thus may be of great importance, given the low serum concentrations. Furthermore, heparin was identified as a first activating cofactor of vaspin. A detailed and better understanding of vaspin action and its regulation, the identification of further proteases targeted by vaspin and identification of the substrates of these proteases, should increase the understanding of the diverse beneficial effects of vaspin and lead to new pharmacologic targets and potentially new treatment strategies for obesity related metabolic and inflammatory diseases.

Author contributions
David Ulbricht, Jan Pippel, Stephan Schultz and John Heiker expressed recombinant proteins and performed experiments; Jan Pippel and Norbert Sträter crystallized proteins and carried out crystal structure determinations; Rene Meier helped with interpretation of data; John Heiker conceived and supervised project, and wrote paper with contributions from all authors.

Acknowledgements The vaspin expression plasmid was kindly provided by Dr. J. Wada (Department of Medicine and Clinical Science Okayama University Graduate School of Medicine, Okayama, Japan). The substrate peptide used in heparin-activation studies was a generous gift of Prof. Dr. Maria A. Juliano (Department of Biophysics, Escola Paulista de Medicina, Universidade Federal de São Paulo, Brazil). We thank Antje Keim for helping with crystallization trials.

Funding This work was funded by the European Union and the Free State of Saxony (J.T.H.) and supported by grants of the German Research Foundation (DFG) within the Collaborative Research Centre SFB1052 “Obesity Mechanisms” (C4 N.S., C7 J.T.H.). The authors thank the Joint Berlin MX-Laboratory at BESSY II, Berlin, Germany, for beam time and assistance during synchrotron data collection as well as the Helmholtz Zentrum Berlin for travelling support.

References

1 Hida, K., Wada, J., Eguchi, J., Zhang, H., Baba, M., Seida, A., Hashimoto, L., Okada, T., Yasuhara, A., Nakatsuka, A., Shikata, K., Hourai, S., Futami, J., Watanabe, E., Matsuki, Y., Hiramatsu, R., Akagi, S., Makino, H. and Kanwar, Y. S. (2005) Visceral adipose tissue-derived serine protease inhibitor: A unique insulin-sensitizing adipocytokine in obesity. Proc. Natl. Acad. Sci. U. S. A. **102**, 10610-10615

2 Kloting, N., Berndt, J., Kralisch, S., Kovacs, P., Fasshauer, M., Schon, M. R., Stumvoll, M. and Bluher, M. (2006) Vaspin gene expression in human adipose tissue: association with obesity and type 2 diabetes. Biochem. Biophys. Res. Commun. **339**, 430-436

3 Youn, B. S., Kloting, N., Kratzsch, J., Lee, N., Park, J. W., Song, E. S., Ruschke, K., Oberbach, A., Fasshauer, M., Stumvoll, M. and Bluher, M. (2008) Serum vaspin concentrations in human obesity and type 2 diabetes. Diabetes. **57**, 372-377

4 Bluher, M. (2012) Vaspin in obesity and diabetes: pathophysiological and clinical significance. Endocrine. **41**, 176-182

5 Heiker, J. T. (2014) Vaspin (serpinA12) in obesity, insulin resistance, and inflammation. J Pept Sci. **20**, 299-306

6 Nakatsuka, A., Wada, J., Iseda, I., Teshigawara, S., Higashio, K., Murakami, K., Kanzaki, M., Inoue, K., Terami, T., Katayama, A., Hida, K., Eguchi, J., Horiguchi, C. S., Ogawa, D., Matsuki, Y., Hiramatsu, R., Yagita, H., Kakuta, S., Iwakura, Y. and Makino, H. (2012) Vaspin is an adipokine ameliorating ER stress in obesity as a ligand for cell-surface GRP78/MTJ-1 complex. Diabetes. **61**, 2823-2832

7 Kloting, N., Kovacs, P., Kern, M., Heiker, J. T., Fasshauer, M., Schon, M. R., Stumvoll, M., Beck-Sickinger, A. G. and Bluher, M. (2011) Central vaspin administration acutely reduces food intake and has sustained blood glucose-lowering effects. Diabetologia. **54**, 1819-1823

8 Heiker, J. T., Kloting, N., Kovacs, P., Kuettner, E. B., Strater, N., Schultz, S., Kern, M., Stumvoll, M., Bluher, M. and Beck-Sickinger, A. G. (2013) Vaspin inhibits kallikrein 7 by serpin mechanism. Cell. Mol. Life Sci. **70**, 2569-2583

9 Eissa, A. and Diamandis, E. P. (2008) Human tissue kallikreins as promiscuous modulators of homeostatic skin barrier functions. Biol. Chem. **389**, 669-680

10 Schultz, S., Saalbach, A., Heiker, J. T., Meier, R., Zellmann, T., Simon, J. C. and Beck-Sickinger, A. G. (2013) Proteolytic activation of prochemerin by kallikrein 7 breaks an ionic linkage and results in C-terminal rearrangement. Biochem. J. **452**, 271-280

11 Saalbach, A., Vester, K., Rall, K., Tremel, J., Anderegg, U., Beck-Sickinger, A. G., Bluher, M. and Simon, J. C. (2012) Vaspin--a link of obesity and psoriasis? Exp. Dermatol. **21**, 309-312

12 Hansson, L., Backman, A., Ny, A., Edlund, M., Ekholm, E., Ekstrand Hammarstrom, B., Tornell, J., Wallbrandt, P., Wennbo, H. and Egelrud, T. (2002) Epidermal overexpression of stratum corneum chymotryptic enzyme in mice: a model for chronic itchy dermatitis. J. Invest. Dermatol. **118**, 444-449

13 Ny, A. and Egelrud, T. (2004) Epidermal hyperproliferation and decreased skin barrier function in mice overexpressing stratum corneum chymotryptic enzyme. Acta Derm. Venereol. **84**, 18-22

14 Psyrri, A., Kountourakis, P., Scorilas, A., Markakis, S., Camp, R., Kowalski, D., Diamandis, E. P. and Dimopoulos, M. A. (2008) Human tissue kallikrein 7, a novel biomarker for advanced ovarian carcinoma using a novel in situ quantitative method of protein expression. Ann. Oncol. **19**, 1271-1277

15 Talieri, M., Diamandis, E. P., Gourgiotis, D., Mathioudaki, K. and Scorilas, A. (2004) Expression analysis of the human kallikrein 7 (KLK7) in breast tumors: a new potential biomarker for prognosis of breast carcinoma. Thromb. Haemost. **91**, 180-186

16 Santin, A. D., Cane, S., Bellone, S., Bignotti, E., Palmieri, M., De Las Casas, L. E., Roman, J. J., Anfossi, S., O'Brien, T. and Pecorelli, S. (2004) The serine protease stratum corneum chymotryptic enzyme (kallikrein 7) is highly overexpressed in squamous cervical cancer cells. Gynecol. Oncol. **94**, 283-288

17 Oliveira, J. R., Bertolin, T. C., Andrade, D., Oliveira, L. C., Kondo, M. Y., Santos, J. A., Blaber, M., Juliano, L., Severino, B., Caliendo, G., Santagada, V. and Juliano, M. A. (2015) Specificity studies on Kallikrein-related peptidase 7 (KLK7) and effects of osmolytes and glycosaminoglycans on its peptidase activity. Biochim. Biophys. Acta. **1854**, 73-83

18 Baglin, T. P., Carrell, R. W., Church, F. C., Esmon, C. T. and Huntington, J. A. (2002) Crystal structures of native and thrombin-complexed heparin cofactor II reveal a multistep allosteric mechanism. Proc. Natl. Acad. Sci. U. S. A. **99**, 11079-11084
19 Chen, V. C., Chao, L. and Chao, J. (2000) A positively charged loop on the surface of kallistatin functions to enhance tissue kallikrein inhibition by acting as a secondary binding site for kallikrein. J. Biol. Chem. **275**, 40371-40377
20 Kabsch, W. (2010) Xds. Acta Crystallogr D Biol Crystallogr. **66**, 125-132
21 Evans, P. R. and Murshudov, G. N. (2013) How good are my data and what is the resolution? Acta Crystallogr D Biol Crystallogr. **69**, 1204-1214
22 Collaborative Computational Project, N. (1994) The CCP4 suite: programs for protein crystallography. Acta Crystallogr D Biol Crystallogr. **50**, 760-763
23 Murshudov, G. N., Skubak, P., Lebedev, A. A., Pannu, N. S., Steiner, R. A., Nicholls, R. A., Winn, M. D., Long, F. and Vagin, A. A. (2011) REFMAC5 for the refinement of macromolecular crystal structures. Acta Crystallogr D Biol Crystallogr. **67**, 355-367
24 Murshudov, G. N., Vagin, A. A. and Dodson, E. J. (1997) Refinement of macromolecular structures by the maximum-likelihood method. Acta Crystallogr D Biol Crystallogr. **53**, 240-255
25 Bricogne, G., Blanc, E., Brandl, M., Flensburg, C., Keller, P., Paciorek, W., Roversi, P., Sharff, A., Smart, O. S., Vonrhein, C. and Womack, T. O. (2011) BUSTER version 2.10.1. . Cambridge, United Kingdom: Global Phasing Ltd.
26 Emsley, P., Lohkamp, B., Scott, W. G. and Cowtan, K. (2010) Features and development of Coot. Acta Crystallogr D Biol Crystallogr. **66**, 486-501
27 Painter, J. and Merritt, E. A. (2006) Optimal description of a protein structure in terms of multiple groups undergoing TLS motion. Acta Crystallogr D Biol Crystallogr. **62**, 439-450
28 Painter, J. and Merritt, E. A. (2006) TLSMD web server for the generation of multi-group TLS models. J Appl Crystallogr. **39**, 109-111
29 Chen, V. B., Arendall, W. B., 3rd, Headd, J. J., Keedy, D. A., Immormino, R. M., Kapral, G. J., Murray, L. W., Richardson, J. S. and Richardson, D. C. (2010) MolProbity: all-atom structure validation for macromolecular crystallography. Acta Crystallogr D Biol Crystallogr. **66**, 12-21
30 Adams, P. D., Afonine, P. V., Bunkoczi, G., Chen, V. B., Davis, I. W., Echols, N., Headd, J. J., Hung, L. W., Kapral, G. J., Grosse-Kunstleve, R. W., McCoy, A. J., Moriarty, N. W., Oeffner, R., Read, R. J., Richardson, D. C., Richardson, J. S., Terwilliger, T. C. and Zwart, P. H. (2010) PHENIX: a comprehensive Python-based system for macromolecular structure solution. Acta Crystallogr D Biol Crystallogr. **66**, 213-221
31 Afonine, P. V., Moriarty, N. W., Mustyakimov, M., Sobolev, O. V., Terwilliger, T. C., Turk, D., Urzhumtsev, A. and Adams, P. D. (2015) FEM: feature-enhanced map. Acta crystallographica. Section D, Biological crystallography. **71**, 646-666
32 Berman, H. M., Westbrook, J., Feng, Z., Gilliland, G., Bhat, T. N., Weissig, H., Shindyalov, I. N. and Bourne, P. E. (2000) The Protein Data Bank. Nucleic Acids Res. **28**, 235-242
33 Horvath, A. J., Irving, J. A., Rossjohn, J., Law, R. H., Bottomley, S. P., Quinsey, N. S., Pike, R. N., Coughlin, P. B. and Whisstock, J. C. (2005) The murine orthologue of human antichymotrypsin: a structural paradigm for clade A3 serpins. J. Biol. Chem. **280**, 43168-43178
34 Ksiazek, M., Mizgalska, D., Enghild, J. J., Scavenius, C., Thogersen, I. B. and Potempa, J. (2014) Miropin, a novel bacterial serpin from the periodontopathogen Tannerella forsythia, inhibits a broad range of proteases by using different peptide bonds within the reactive center loop. J. Biol. Chem. **290**, 658-670
35 Schechter, N. M., Jordan, L. M., James, A. M., Cooperman, B. S., Wang, Z. M. and Rubin, H. (1993) Reaction of human chymase with reactive site variants of alpha 1-antichymotrypsin. Modulation of inhibitor versus substrate properties. J. Biol. Chem. **268**, 23626-23633
36 Greenfield, N. J. (1996) Methods to estimate the conformation of proteins and polypeptides from circular dichroism data. Anal. Biochem. **235**, 1-10
37 Gettins, P. G. (2002) Serpin structure, mechanism, and function. Chem. Rev. **102**, 4751-4804
38 Gettins, P. G. and Olson, S. T. (2009) Exosite determinants of serpin specificity. J. Biol. Chem. **284**, 20441-20445
39 Chen, V. C., Chao, L., Pimenta, D. C., Bledsoe, G., Juliano, L. and Chao, J. (2001) Identification of a major heparin-binding site in kallistatin. The Journal of biological chemistry. **276**, 1276-1284

40 Huntington, J. A. and Gettins, P. G. (1998) Conformational conversion of antithrombin to a fully activated substrate of factor Xa without need for heparin. Biochemistry (Mosc). **37**, 3272-3277
41 Irving, J. A., Haq, I., Dickens, J. A., Faull, S. V. and Lomas, D. A. (2014) Altered native stability is the dominant basis for susceptibility of alpha1-antitrypsin mutants to polymerization. Biochem. J. **460**, 103-115
42 Irving, J. A., Cabrita, L. D., Rossjohn, J., Pike, R. N., Bottomley, S. P. and Whisstock, J. C. (2003) The 1.5 A crystal structure of a prokaryote serpin: controlling conformational change in a heated environment. Structure. **11**, 387-397
43 Bruce, D., Perry, D. J., Borg, J. Y., Carrell, R. W. and Wardell, M. R. (1994) Thromboembolic disease due to thermolabile conformational changes of antithrombin Rouen-VI (187 Asn-->Asp). J. Clin. Invest. **94**, 2265-2274
44 Mottonen, J., Strand, A., Symersky, J., Sweet, R. M., Danley, D. E., Geoghegan, K. F., Gerard, R. D. and Goldsmith, E. J. (1992) Structural basis of latency in plasminogen activator inhibitor-1. Nature. **355**, 270-273
45 Carrell, R. W., Stein, P. E., Fermi, G. and Wardell, M. R. (1994) Biological implications of a 3 A structure of dimeric antithrombin. Structure. **2**, 257-270
46 Yamasaki, M., Sendall, T. J., Pearce, M. C., Whisstock, J. C. and Huntington, J. A. (2011) Molecular basis of alpha1-antitrypsin deficiency revealed by the structure of a domain-swapped trimer. EMBO Rep. **12**, 1011-1017
47 Lomas, D. A., Evans, D. L., Finch, J. T. and Carrell, R. W. (1992) The mechanism of Z alpha 1-antitrypsin accumulation in the liver. Nature. **357**, 605-607
48 Patston, P. A., Hauert, J., Michaud, M. and Schapira, M. (1995) Formation and properties of C1-inhibitor polymers. FEBS Lett. **368**, 401-404
49 Jeong, E., Youn, B. S., Kim, D. W., Kim, E. H., Park, J. W., Namkoong, C., Jeong, J. Y., Yoon, S. Y., Park, J. Y., Lee, K. U. and Kim, M. S. (2010) Circadian rhythm of serum vaspin in healthy male volunteers: relation to meals. J. Clin. Endocrinol. Metab. **95**, 1869-1875
50 Kovacs, P., Miehle, K., Sandner, B., Stumvoll, M. and Bluher, M. (2013) Insulin administration acutely decreases vaspin serum concentrations in humans. Obes Facts. **6**, 86-88

Figure Legends

Figure 1. Crystal structure of human vaspin and mutants vaspin E379S and D305C/V383C. (**A**) Structure of human vaspin (pdb 4IF8) with β-strands and loops shown in cyan and α-helices in red. The dotted black line indicates flexible and unresolved RCL residues. The detailed view of the RCL-s2C interactions is from the back left with residues 301-302 (s2C), 378-384 (RCL) shown as sticks and selected molecules as spheres. The feature enhanced electron density map calculated with PHENIX is displayed at 1 σ contour level in red. (**B**) Feature enhanced maps of RCL and selected s2C residues of vaspin E379S contoured at 1 s. (**C**) corresponding residues of the D305C/V383C variant also demonstrating successful formation of the introduced disulfide bond. To more clearly present electron density of RCL residues and the disulfide bond, note that the view point for (B) and (C) is slightly rotated to the left compared to (A).

Figure 2. Kinetic analysis for the inhibition of KLK7 by vaspin and mutants. (**A**) Stoichiometry of inhibition was determined by linear regression to extrapolate the inhibitor to enzyme (I_0/E_0) ratio for complete loss of KLK7 activity. (**B**) Inhibition of KLK7 by vaspin wt and mutants D305C/V383C, R302E/E379S and R302A were measured under pseudo-first-order conditions in a discontinuous assay using at least six different inhibitor concentrations. The k_a was determined as the slope of the linear fit after plotting k_{obs} vs. I_0. (**C**) KLK7 inhibition by vaspin E379S was determined by using the progress curve method. KLK7 inactivation was monitored for 45 min and k_{obs} was calculated by a non-linear regression fit of each curve. Accounting for K_m of KLK7 for the peptide substrate, the slope of k_{obs} vs. I_0 resulted in the k_a. The mean values of at least three experiments are reported in Table 2.

Figure 3. Complex formation analyses of vaspin wild-type and mutants with KLK7 by SDS-PAGE. (**A**) Coomassie stained SDS-gels of vaspin wild-type (wt) and mutants D305C/V383C and E379S incubated with KLK7 for indicated times and respective control samples without protease. (**B**) Respective Coomassie stained gels for mutants R302A and R302E incubated with KLK7. (**C**) RP-HPLC monitoring of synthetic vaspin RCL comprising peptide vaspin(365-388) incubated with or without KLK7 reveals no detectable cleavage (linear gradient of ACN/H_2O from 10-50 % in 40 min). (**D**) Coomassie stained gels for mutants R302A/D305C/V383C, R302E/D305C/V383C and R302E/E379S incubated with KLK7. Notable and indicated bands are: 1 - serpin-protease complex; 2 - active serpin; 3 - active, Tag-cleaved serpin; 4 - cleaved serpin; 5 - protease.

Figure 4. Heparin binding and activation of vaspin. (**A**) Elution profiles of recombinant wt vaspin and KLK7 by heparin-affinity chromatography using a NaCl gradient (black dotted line) monitored at 220 nm. Vaspin elutes at ~580 mM, KLK7 at 420 mM NaCl. (**B**) Analysis of concentration dependent heparin accelerated complex formation of vaspin and KLK7. Coomassie stained SDS-gel of a fixed molar ratio (1:3) of vaspin wild-type (wt) and KLK7 incubated with increasing concentrations of unfractionated heparin (0.1–100-fold vaspin) for 1 min and a reference sample without heparin (0x). The control (con) is vaspin and heat-inactivated KLK7. (**C**) Densitometric quantification of complex band intensities in relation to the molar ratio of unfractionated heparin (ufh) to vaspin of SDS-gels as in (B). A bell-shaped curve is obtained suggesting the bridging mechanism as the major contribution to heparin activation of vaspin. (**D**) Inhibition of KLK7 by vaspin wt with different concentrations of unfractionated heparin was measured under pseudo-first-order conditions in a discontinuous assay. Presented is the increase in second order rate constant in x-fold over control (without heparin). The k_a values were determined as described in Materials and methods.

Figure 5. Thermo-stability and heat-induced polymerization of vaspin wild-type and mutants. (**A**) Far-UV CD spectra of vaspin wild-type (wt) and mutants D305C/V383C, E379S, R302A and R302E at 20 °C are shown (collected in phosphate buffer, pH 7.8, 1.5 μM). (**B**) CD spectra of vaspin at different stages of thermal denaturation from a single sample. (**C**) Thermal unfolding of vaspin and mutants from single samples observed by far-UV CD at 208 nm at a heating rate of 50 °C/h. (**D**) SDS-PAGE analysis of vaspin-KLK7 complex formation or (**E**) vaspin and ATIII polymerization after incubation at 60 °C for indicated times. (**F**) Heat-induced polymerization for wild-type vaspin and R302A, R302E, E379S, R302E/E379S and D305C/V383C variants after incubation at 70 °C for up to 60 min. Mutation of Arg^{302} significantly increases polymer formation.

Table 1: Details of the crystal structure analysis

	vaspin D305C/V383C	vaspin E379S
Crystallization and data collection		
Crystallization buffer	6 % (w/v) polyethylene glycol 6000, 0.1 M citric acid pH 3.5–4.5	2.5 M ammonium sulfate, 0.1 M sodium citrate pH 4.0–4.6
Crystallization drop	1 µL crystallization buffer +1µL of 6 mg/mL protein in 50 mM Tris pH 7.5, 150 mM NaCl	1µL crystallization buffer +1µL of 10.2 mg/mL protein in 50 mM Tris pH 7.5, 150 mM NaCl, 0.52 mM heparin tetrasaccharide dp4
Cryobuffer	Crystallization buffer +20 % (v/v) ethylene glycol	Crystallization buffer +20 % (v/v) ethylene glycol
Wavelength (Å)	0.91841	0.91841
Resolution range (Å)[1]	19.69 - 2.2 (2.26 - 2.2)	48.37 - 2.2 (2.26 - 2.2)
Space group	C2	C2
Unit cell parameters a, b, c (Å), α, β, γ (°)	133.5, 152.3, 61.6, 90, 97.1, 90	133.0, 151.4, 61.6, 90, 98.4, 90
Total reflections[1]	342549 (19778)	208807 (15788)
Unique reflections[1]	61536 (4375)	60841 (4481)
Multiplicity[1]	5.6 (4.5)	3.4 (3.5)
Completeness (%)[1]	99.6 (96.3)	99.8 (99.8)
Mean I/sigma(I) [1]	7.9 (0.9)	7.2 (0.9)
R-merge[1]	0.145 (1.554)	0.125 (1.413)
R-pim[1]	0.067 (0.798)	0.080 (0.885)
CC1/2[1]	0.996 (0.285)	0.996 (0.206)
CC*[1]	0.999 (0.666)	0.999 (0.584)
Wilson B-factor (Å^2)	46.70	45.62
Monomers/asymmetric unit	2	2
Refinement		
R-work[1]	0.1801 (0.2251)	0.1862 (0.2485)
R-free[1]	0.2058 (0.2406)	0.2193 (0.2574)
Protein residues	727 (chain A: 36-366, 380-414; chain B: 34-277, 281-365, 382-413)	728 (chain A: 35-367, 381-414; chain B: 35-277, 280-365, 383-414)
Number of non-hydrogen atoms		
Total	6237	6224
Protein	5949	5983
Ligands	33	53
Water	255	188

Rmsd		
Bonds (Å)	0.009	0.010
Angles (°)	1.08	1.12
Ramachandran statistics		
Favored (%)	96.54	95.87
Allowed (%)	3.46	4.13
Outliers (%)	0	0
B-factor (Å^2)		
Average	66.445	71.939
Protein	66.879	72.616
Chain A	55.418	56.266
Chain B	78.553	89.148
Ligands	60.858	59.968
Water	57.038	53.758

[1]values in parenthesis correspond to highest resolution shell

Table 2. Kinetic parameters for the inhibition of KLK7 by vaspin and mutants

Vaspin variant	k_a	SI
	$mM^{-1}\ s^{-1}$	*I / E (mol / mol)*
wild-type	12.3 ± 0.3	3.6 ± 0.3
D305C/V383C	56.9 ± 9.7	2.0 ± 0.2
E379S	403.0 ± 34.4	2.0 ± 0.1
R302A	0.3 ± 0.1	2.7 ± 0.6*
R302E	0.03	3.2 ± 0.2*
R302E/E379S	20.7 ± 4.2	3.2 ± 0.2

*densitometric estimation; I Inhibitor; E Enzyme; Data presented as averages of at least three experiments ± S.D. with exception of k_a for R302E.

FIGURE 1

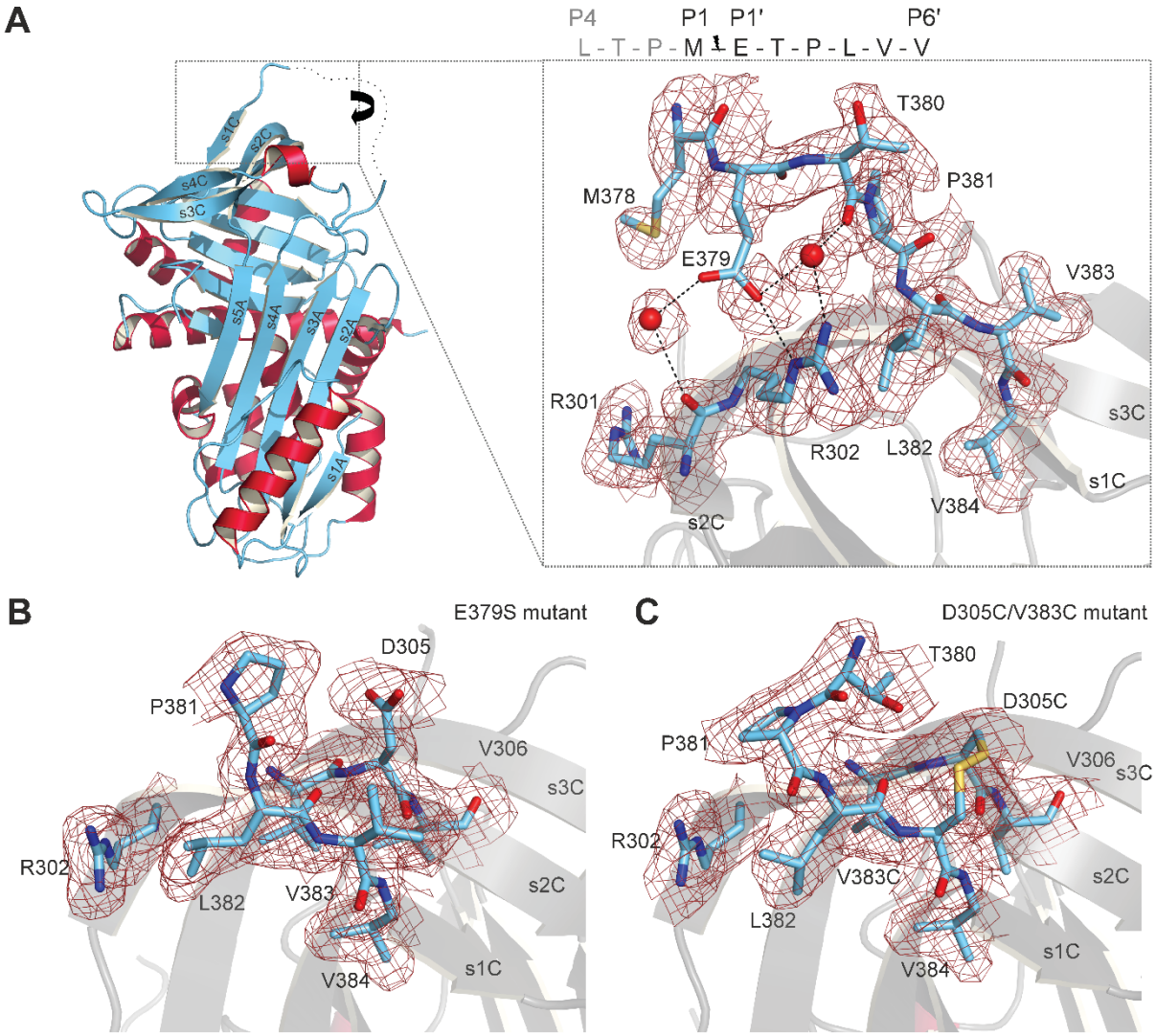
A
P4 P1 P1' P6'
L - T - P - M - E - T - P - L - V - V
s1C
s2C
s4C
s3C
s5A
s4A
s3A
s2A
s1A
T380
P381
M378
E379
V383
R301
s3C
R302
L382
s1C
V384
s2C
B
E379S mutant
D305
P381
V306
s3C
R302
s2C
L382
V383
s1C
V384
C
D305C/V383C mutant
T380
D305C
P381
V306
s3C
R302
s2C
V383C
L382
s1C
V384

FIGURE 2

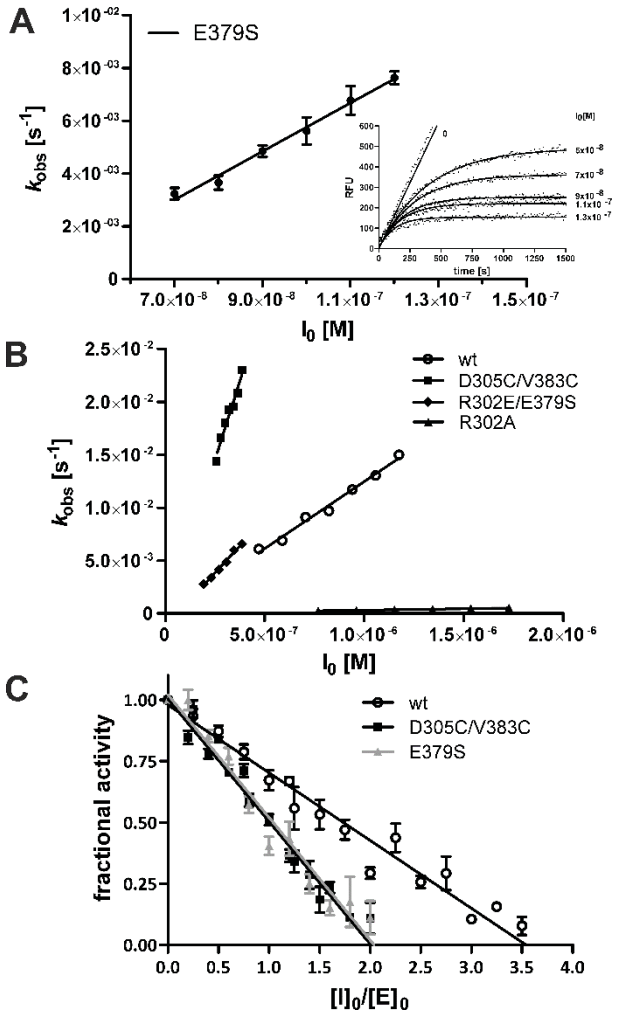
A
E379S
k_{obs} [s^{-1}]
I_0 [M]
RFU
time [s]
B
wt
D305C/V383C
R302E/E379S
R302A
k_{obs} [s^{-1}]
I_0 [M]
C
wt
D305C/V383C
E379S
fractional activity
$[I]_0/[E]_0$

FIGURE 3

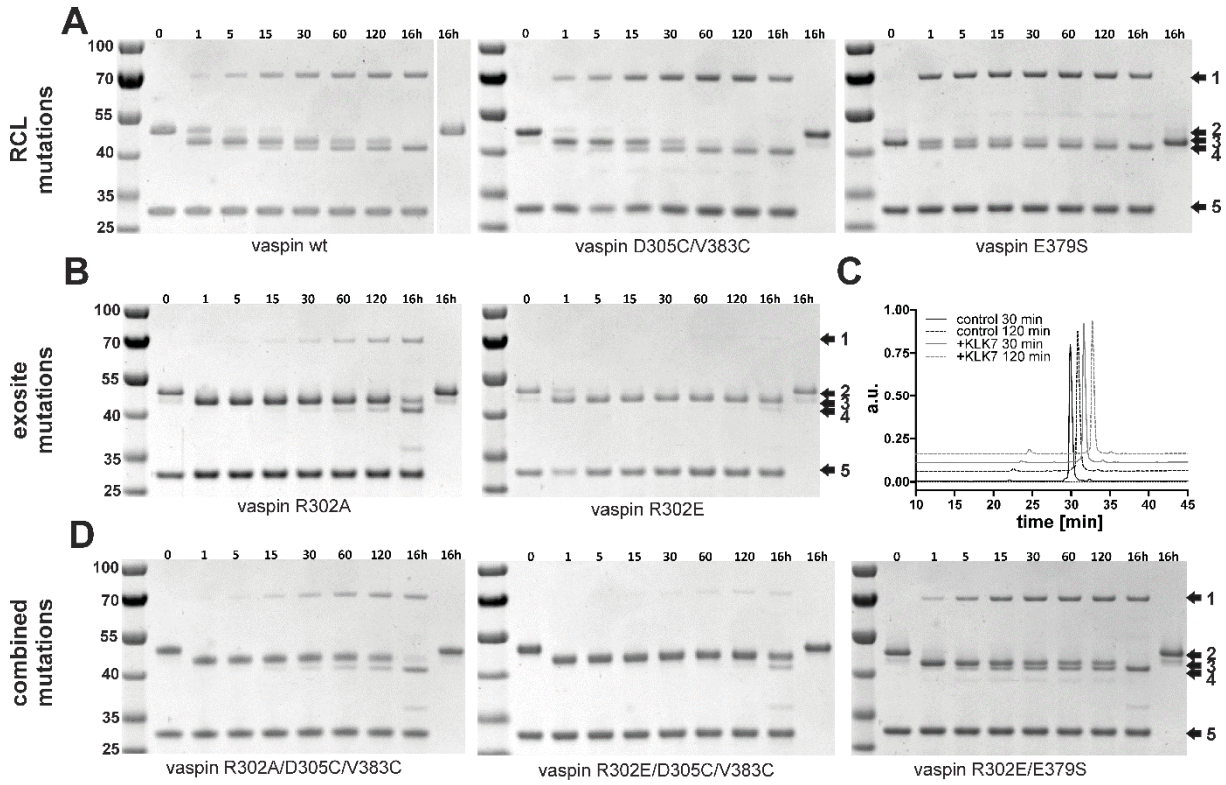
A
RCL mutations
0 1 5 15 30 60 120 16h 16h
100
70
55
40
35
25
vaspin wt
vaspin D305C/V383C
vaspin E379S
1
2
3
4
5
B
exosite mutations
vaspin R302A
vaspin R302E
C
control 30 min
control 120 min
+KLK7 30 min
+KLK7 120 min
a.u.
1.00
0.75
0.50
0.25
0.00
10 15 20 25 30 35 40 45
time [min]
D
combined mutations
vaspin R302A/D305C/V383C
vaspin R302E/D305C/V383C
vaspin R302E/E379S

FIGURE 4

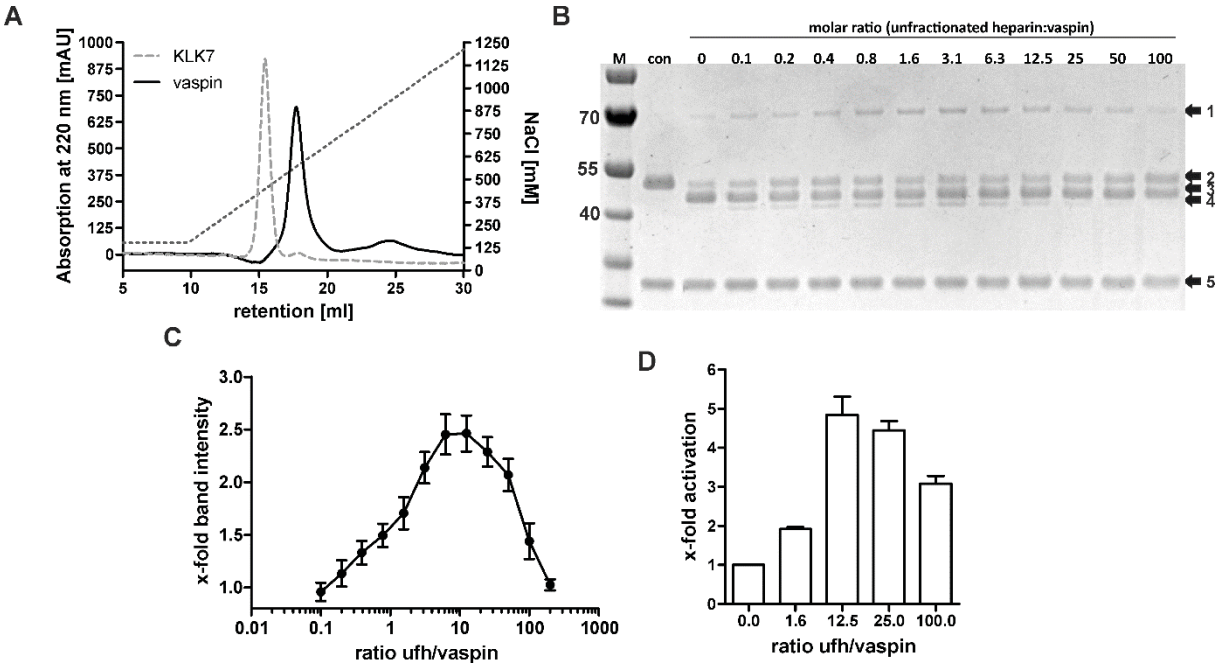
A
Absorption at 220 nm [mAU]
KLK7
vaspin
NaCl [mM]
retention [ml]
B
molar ratio (unfractionated heparin:vaspin)
M
con
0
0.1
0.2
0.4
0.8
1.6
3.1
6.3
12.5
25
50
100
70
55
40
1
2
3
4
5
C
x-fold band intensity
ratio ufh/vaspin
D
x-fold activation
0.0
1.6
12.5
25.0
100.0
ratio ufh/vaspin

FIGURE 5

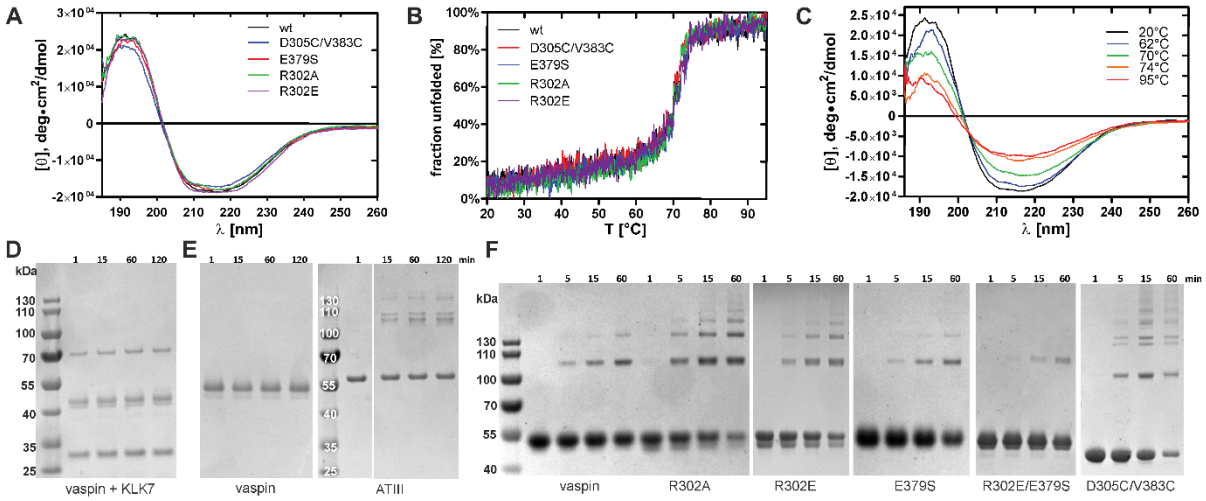
A
wt
D305C/V383C
E379S
R302A
R302E
[θ], deg•cm²/dmol
λ [nm]
B
wt
D305C/V383C
E379S
R302A
R302E
fraction unfolded [%]
T [°C]
C
20°C
62°C
70°C
74°C
95°C
[θ], deg•cm²/dmol
λ [nm]
D
kDa
vaspin + KLK7
E
vaspin
ATIII
min
F
kDa
vaspin
R302A
R302E
E379S
R302E/E379S
D305C/V383C
min